Acta Geotechnica
DOI 10.1007/s11440-008-0065-0

RESEARCH PAPER

PreMDB, a thermodynamically consistent material database as a key to geodynamic modelling

D. Siret · T. Poulet · K. Regenauer-Lieb · J. A. D. Connolly

Received: 29 September 2007 / Accepted: 29 February 2008

Abstract We present a tool for coupling thermochemistry with mechanics. Thermodynamic potential functions are used to calculate reversible material properties such as thermal expansion coefficient, specific heat, elastic shear modulus, bulk modulus and density. These material properties are thermodynamically self consistent. Transport properties such as thermal conductivity (diffusivity) and melt viscosity are also included, but these are derived from laboratory experiments. The transport properties are included to provide a reference database as a common standard of material properties necessary for comparing geological, geodynamic and geotechnical calculations. We validate the chemically derived elastic material properties by comparing computed seismic velocities for a pyrolitic composition to the seismic models PREM and ak135.

Keywords Earth structure · Elastic constants · Numerical modelling · Reference material database · Seismic velocities · Thermodynamics

D. Siret (✉) · T. Poulet · K. Regenauer-Lieb
CSIRO Exploration and Mining Division,
26 Dick Perry Avenue, Kensington, WA 6151, Australia
e-mail: Delphine.Siret@csiro.au

K. Regenauer-Lieb
Earth and Geographical Sciences,
The University of Western Australia,
35, Stirling Highway,
Crawley, WA 6009, Australia

J. A. D. Connolly
Earth Science Department,
Swiss Federal Institute of Technology,
8092 Zurich, Switzerland

1 Introduction

Material properties are essential to realistic simulations of geodynamic and geological processes. These properties generally derive from laboratory experiments and geophysical observations [3, 5, 6, 12, 13, 22, 23, 29, 36, 43, 46]. Additionally, numerical data calculated from thermodynamic potentials are a complement to empirical data [24, 25, 40, 44]. There has been considerable progress in geodynamic, thermodynamic and petrological modelling [9, 11, 29, 40, 41]. Here, we present a tool for coupling thermochemistry with mechanics. The main purpose of this tool is to provide geodynamicists and seismologists easy access to thermochemistry.

The thermodynamic equilibrium problem as solved by Gibbs energy minimisation determines the basic mechanical properties needed for geophysics and geodynamics. Reversible material properties such as the thermal expansion coefficient, specific heat, elastic shear modulus, bulk modulus and density can thus be obtained self-consistently, in a thermodynamic sense. It follows that thermodynamic potential functions can be used to model geodynamical processes. Specifically, density differences driving for instance subduction do not need to be assigned but follow from chemical composition and temperature. Moreover, reversible material property changes at phase transitions can trigger events that may be of interest to the geodynamicists and seismologists [4].

Previous works on thermodynamically derived material data have been presented in the seismic tomographic community with the focus of solving the inverse problem for chemistry from seismic velocities [5, 14, 46]. These models gather a collection of physical properties from independent sources and are not thermodynamically self-consistent as pointed out by several authors [9, 10, 41].

Stixrude and Lithgow-Bertelloni [41] have extended the thermodynamic formulation by tensorial presentation of stress and the relationship to entropy and temperature. Therefore, the elastic shear modulus is derived without ad hoc assumptions. This formulation, among others, is implemented in the software Perple_X [9] which permits extraction of any thermodynamic property as a generalised formulation of temperature, pressure and composition.

Other codes have also been put forward (ThermoCalc, Domino, FreeGs) with different thermodynamic solvers that focus on determining phase equilibria in petrological systems regardless of the self consistency of material properties. These codes use non-linear techniques for Gibbs energy minimisation. The strength of these non-linear methods is their accuracy. However their weakness is that identification of the stable mineral assemblage is probable but not certain. This lack of robustness obviates the use of non-linear methods for embedded geodynamic calculations. In contrast, Perple_X utilises a linearised formulation of the minimisation problem which always converges [8, 9, 11]. For the derivation of self consistent material properties, this linearised algorithm is convenient because it minimizes data gaps. Another important aspect is that for the purpose of deriving material data the best strategy is to reject mixed formulations, where discrepancies with field observations are adjusted without changing the underlying basic entropy model. Emergence of thermodynamic solvers for geodynamic processes thus puts a strong constraint on basic consistency of the dataset. All these reasons lead us to use Perple_X. We present here a reference database for the purpose of standardising material properties to be used particularly in geological, geodynamic and geotechnical calculations. The numerical results have been validated by comparing seismic velocities predicted for a pyrolitic composition to the seismic models PREM [15] and ak135 [26, 32]. These models, constructed after travel time data, give access to detailed information about the average Earth's structure.

2 Methods

The purpose of PreMDB is to provide modellers with a complete and easy access to fundamental material data for terrestrial rocks and minerals. Another goal is to standardise material data in order to compare results from various numerical and experimental techniques. In order to satisfy these requirements, thermodynamically consistent data have been chosen as they are defined over a large range of temperature and pressure and provide an important complement to experiments and observations. Non-thermodynamic data such as transport or ad hoc properties have also been added. Currently, PreMDB lists 20 material properties for each rock and mineral (Table 1).

In isothermal-isobaric closed chemical system composed of Π phases, the phase equilibria are determined minimising the Gibbs free energy of the system (G^{sys}). This thermodynamic function is a function of temperature (T), pressure (P) and the chemical composition of the system [9, 10]. It is defined as:

$$G^{\mathrm{sys}}(P,T,n) = \sum_{i}^{p} n_i G_i^m(P,T,x_i^1,x_i^2,\ldots,x_i^c) \tag{1}$$

where G_i^m and n_i are respectively the molar Gibbs energy and the number of moles of phase i; x_i^j is the composition of the i^{th} phase with respect to the j^{th} component of the system.

In Perple_X, all reversible material properties are related to the thermodynamic potentials G:

- Entropy S

$$S = -\left(\frac{\partial G}{\partial T}\right)_P \tag{2}$$

- Isochemical enthalpy H

$$H = G + TS \tag{3}$$

- Internal energy U

$$U = H - PV \tag{4}$$

V being the volume.

- Heat capacity C_P

$$C_P = -T\left(\frac{\partial^2 G}{\partial T^2}\right)_P \tag{5}$$

- Density ρ

$$\rho = \frac{N}{V} = N\frac{\partial G}{\partial P} \tag{6}$$

where N is the molar formula weight.

- Thermal expansion α

$$\alpha = -\frac{1}{V}\left(\frac{\partial S}{\partial P}\right)_P = \frac{1}{V}\left(\frac{\partial^2 G}{\partial P \partial T}\right) \tag{7}$$

- Compressibility β

$$\beta = -\frac{1}{V}\left(\frac{\partial^2 G}{\partial P^2}\right)_T \tag{8}$$

- Adiabatic bulk modulus K_s

$$K_s = -\frac{\partial G}{\partial P}\left[\frac{\partial^2 G}{\partial P^2} + \left(\frac{\partial}{\partial P}\frac{\partial G}{\partial T}\right)^2 \Big/ \frac{\partial^2 G}{\partial T^2}\right]^{-1} \tag{9}$$

- Grüneisen parameter γ

Table 1 Physical properties available in PreMDB

Properties calculated in Perple_X	Symbol	Units	Thermodynamic-consistent	
			S&LB model[a]	Other models
Enthalpy	h	J/kg	✔	✔
Specific enthalpy	$h \times \rho$	J/m^3	✔	✔
Entropy	s	J/K/kg	✔	✔
Specific entropy	$s \times \rho$	J/K/m^3	✔	✔
Heat capacity	c	J/K/kg	✔	✔
Specific heat	$c \times \rho$	J/K/m^3	✔	✔
Density	ρ	kg/m^3	✔	✔
Thermal expansion	α	1/K	✔	✔
Compressibility	β	1/Pa	✔	✔
Bulk sound velocity	V_Φ	km/s	✔	✔
P-wave velocity	V_P	km/s	✔	
S-wave velocity	V_S	km/s	✔	
Bulk modulus	K_S	GPa	✔	✔
Shear modulus	μ	GPa	✔	
Elastic modulus	E	GPa	✔	
Poisson's ratio	v	–	✔	
Gruneisen ratio	γ	–	✔	✔
Additional transport properties				
Thermal conductivity	k	W/K/m		
Thermal diffusivity	κ	m^2/s		
Melt viscosity	η	Pa.s		

[a] The equations of state describing the solutions are from [3, 6, 10, 14]

$$\gamma = V\left(\frac{\partial P}{\partial U}\right)_V \tag{10}$$

Connolly and Kerrick [10] use an ad hoc empirical model (see equation 5 in [10]) to calculate the shear modulus. Stixrude and Lithgow-Bertelloni' [41] formulation of Gibbs energy for isotropic material permits to relate the shear and elastic moduli to thermodynamic potentials:

- Elastic compliance tensor s_{ijkl}

$$s_{ijkl} = -\frac{1}{V}\frac{\partial^2 G}{\partial\varepsilon_{ij}\partial\varepsilon_{kl}} \tag{11}$$

where $\partial\varepsilon_{ij}$ is the Eulerian elastic strain tensor. The elastic compliance tensor describes the general elastic material behaviour in compression and shear. For an isotropic body there are two independent quantities, e.g. bulk and shear moduli. For anisotropic assemblages of phases, the shear modulus is essentially interpreted as that of an isotropic polycrystalline aggregate.

- Shear modulus μ

$$\frac{1}{\mu} = \frac{1}{V}\sum_{\psi}^{n}\left(x_\psi V_\psi \frac{1}{\mu_\psi}\right) \tag{12}$$

For any equations of state other than those of Stixrude and Lithgow-Bertelloni [40, 41], the shear modulus calculated in Perple_X is not computed self-consistently from thermodynamic potentials [10].

For isotropic elasticity the elastic modulus, as well as seismic properties are obtained from the following equations:

- Elastic modulus E

$$E = \frac{9K_s\mu}{3K_s + \mu} \tag{13}$$

- Poisson's ratio v

$$v = \frac{3K_s - 2\mu}{6K_s + 2\mu} \tag{14}$$

- Bulk sound velocity V_Φ [24]

$$V_\Phi = \sqrt{\frac{K_s}{\rho}} \tag{15}$$

- S-wave velocity V_S

$$V_\mathrm{S} = \sqrt{\frac{\mu}{\rho}} \tag{16}$$

- P-wave velocity V_P

$$V_P = \sqrt{\frac{K_s + 4/3\mu}{\rho}} \tag{17}$$

Seismic wave velocities in a single crystal are thermodynamically self-consistent. On the contrary, they are not in an aggregate of crystals and must be obtained by an ad-hoc averaging scheme such as the Voight-Reuss-Hill theory [10, 45].

Transport properties are estimated from empirical models that are derived from laboratory experiments and expressed as functions of the computed thermodynamic properties:

- Thermal conductivity k

Two equations have been implemented in PreMDB to define k:

- As a function of the temperature T

$$k = A + \frac{B}{350 + T} \tag{18}$$

  where constants A and B are defined for different rock types. k is expressed in n W/m/K and T in Celsius [7, 47].
- As a function of the P-wave velocity V_P

$$k = 0.0681e^{(0.0006V_P)} \tag{19}$$

  with k in W/m/K, V_P in m/s [33].
- Thermal diffusivity κ

$$\kappa = \frac{k}{\rho C_P} \tag{20}$$

  where k is defined according to (Eq. 19), ρ and C_P derived from Perple_X.
- Melt viscosity η

$$\eta = A + \frac{B}{T} + \exp\left(C + \frac{D}{T}\right) \tag{21}$$

where A, B, C and D are linear functions of mole fractions of oxide components, except for H_2O [21].

Depending on the complexity of the system and the precision required, the linearised Gibbs energy minimisation problem can be time consuming. For this reason, computed phase diagram sections and material properties are stored in the PreMDB database. At present compositions of 48 major rock forming dry and wet minerals and 9 terrestrial rocks have been incorporated, representing a standard for the sedimentary part of the crust [34], the upper and lower continental crust [37, 42], the oceanic crust [39] and the mantle (pyrolite and peridotite) [18, 35]. The rocks and minerals currently described in PreMDB are listed in Table 2.

Table 2 Terrestrial rocks and minerals available in PreMDB

Minerals		Rocks		
Dry (25)	Wet (22)	Composition (10)	Water content	References
Albite	Amesite	Sediment	Wet	[3]
Almandine	Annite	Granite	Dry/wet	[6]
Anorthite	Anthophyllite	Granitoid	Dry/wet	[1]
Cordierite	Antigorite	Basalt	Wet	[5]
Diopside	A-phase	Gabbro	Wet	[1]
Enstatite	Brucite	Peridotite	Dry/wet	[2]
Fayalite	Celadonite	Pyrolite	Dry	[4]
Fe-Cordierite	Clinochlore			
Ferrosilite	Daphnite			
Forsterite	Eastonite			
Grossular	Fe-Anthophyllite			
Hedenbergite	Fe-Celadonite			
Hematite	Ferroactinolite			
Hercynite	Glaucophane			
Ilmenite	Hydrous Cordierite			
Jadeite	Margarite			
Kalsilite	Muscovite			
Microcline	Paragonite			
Nepheline	Pargasite			
Pyrope	Phlogopite			
Quartz	Talc			
Sanidine	Tremolite			
Sapphirine442				
Sapphirine793				
Spinel				

A graphical user interface has been developed to browse the database and plot all properties as 2D graphs. The visual representation of all properties is an important role of PreMDB as it is generally cumbersome to interpret or validate data in a tabulated format directly from text files as Perple_X produces them. Reversible properties computed from Perple_X can be visualised as a scale coloured 2D map function of temperature and pressure. Transport properties are either visualised the same way (thermal conductivity derived from Eq. 19 and diffusivity from Eq. 20) or represented as functions of the temperature (thermal conductivity from Eq. 18 and melt viscosity from Eq. 21). Source (Perple_X/equation) and references of each property are presented in the graphical interface. Python (http://www.python.org) is used as a scripting language to post process Perple_X' data and convert them to our own internal data structure. The graphical user

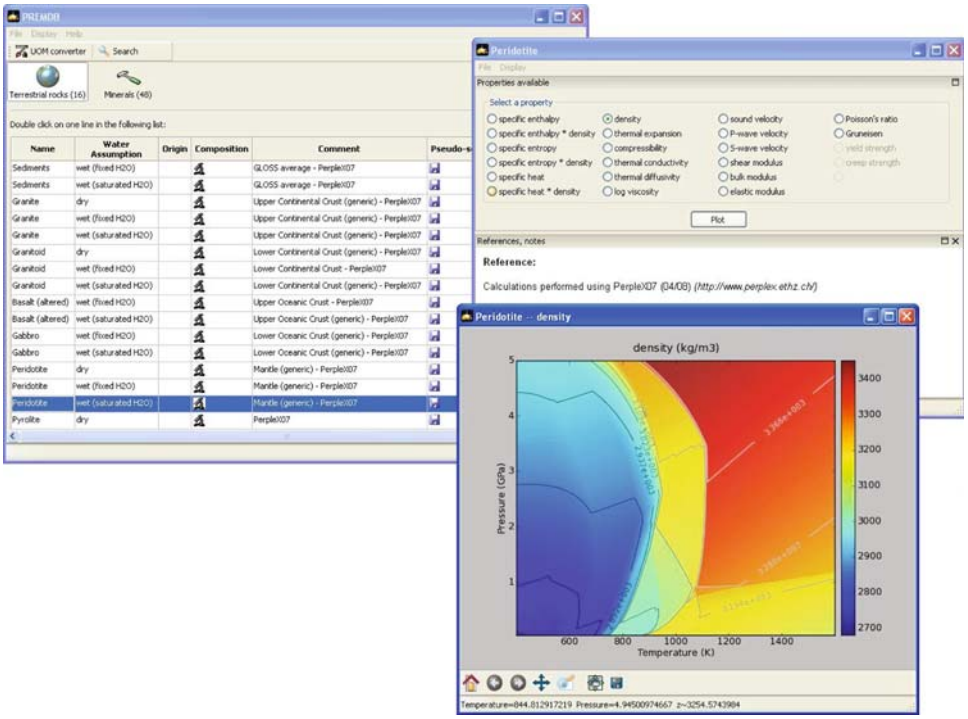

Fig. 1 Example of PreMDB's GUi showing a wet peridotite composition saturated in H_2O. The major density jumps reflect dewatering reactions predicted from thermodynamic modelling

interface is implemented with wxPython (http://www.wxpython.org) and the plots are rendered with Matplotlib (http://matplotlib.sourceforge.net/).

PreMDB's main window lists all materials of the database regrouped by categories under different tabs. There are currently two categories: earth materials and major rock forming minerals. Each category displays a table listing sequentially different rocks/minerals along with their name, composition, comments, Perple_X input files (when applicable) and resulting pseudo-sections. Double clicking on a rock/mineral line opens a new window composed of two distinct parts. The first one lists all material properties available and the second one displays extra information and references on any property selected. Select a property to visualise it. In the case of transport properties, an option is offered for each available equation. The visualisation pops up in another window as the graphical representation of the underlying equation or tabulated data (Fig. 1). Basic functionalities are then available, for instance to magnify the picture, obtain data values under the mouse in the status bar or save the pictures in different file formats. It is possible to open up as many windows as needed to easily compare properties of one or several materials. The main window also displays a toolbar with a unit converter and search functionality.

3 Results

Comparison of petrological data between Perple_X and other thermodynamical softwares has been presented elsewhere [20]. We focus here on the validation of the simulated material properties comparing thermodynamic results to independent sources. The focus of this first presentation of PreMDB is on bulk material properties not on individual mineral data, which will be done in a future contribution. Standard rock compositions are assemblages of different minerals and their properties here are derived from averaging of these constituents. Moreover, simulations calculate ideal rock phase diagrams at thermodynamic equilibrium. Therefore, because of the large variability of rock composition and natural inhomogeneities, it is impossible to perform an exact one to one comparison with a real rock. Another limitation to the validation procedure is that material property data are conventionally derived at ambient laboratory temperature and pressure conditions while thermodynamic simulations cover an extended *T*–*P* range. Therefore, we focus here on a comparison with PREM [15] and ak135 [26, 32] models for the Earth's mantle, down to the core-mantle boundary. To assess the influence of chemistry on seismic properties, three pyrolitic compositions have been considered presenting variable Al_2O_3, CaO and FeO

contents [35, 38, 40]. These compositions are respectively named "Sax", "Rng" and "Stx". Calculations have been performed using the thermodynamic datafile developed by Stixrude and Lithgow-Bertelloni [40] and augmented for the lower mantle as described by Khan et al. [27].

Both seismic models PREM and ak135 have been constructed from travel time data. These 1D models provide a good description of the elastic moduli of the mantle, but inferring average temperature and composition from them requires a model of the equation of state (EoS) and accurate knowledge of the thermoelastic properties of minerals. For the purpose of the comparison to seismic datasets, we calculate the temperature in the mantle self-consistently following an approach proposed by Ita and Stixrude [24]. We assume an adiabatic interior overlain by a lithosphere defined by the half-space conductive cooling solution. We chose to consider a potential temperature of 1,600K for the 100 Ma geotherm as this temperature lies between two estimates of potential temperature required to produce oceanic crust of average thickness [28, 31]. The isentrope is computed self-consistently by finding the P–T path along which the total entropy of the assemblage is constant. While the isentropic assumption follows the principle of self-consistency, we do not argue that the mantle is isentropic.

We compare the density, P- and S-wave velocity and Poisson's ratio adopted in the seismic models PREM and ak135 to the one calculated for pyrolite mantle composition with varying Al_2O_3, CaO and FeO contents (Figs. 2, 3, 4, 5). We obtain global agreement between seismological and thermochemical models (autocorrelation functions ACF respectively varying between 0.996–0.998, 0.996–0.998, 0.988–0.995 and 0.748–0.779 for PreMDB/PREM and 0.992–0.996, 0.994–0.997, 0.987–0.994 and 0.763–0.782 for PreMDB/ak135), except for the Poisson's ratio. The discrepancy for this parameter results from the square root relation between the P- and S-wave velocity ratio (V_P/V_S) and the Poisson's ratio (v):

$$\frac{V_P}{V_S} = \sqrt{\frac{2(1-v)}{1-2v}} \tag{22}$$

Therefore, the deviation for this latter parameter is squared, making the Poisson's ratio more sensitive to chemistry.

The mixture of 60% of pyrolitic and 40% of chondritic composition proposed by Matas et al. [29] has also been tested but did not fit any better the seismic models.

A robust result of our comparison is that the low-velocity layer underneath the lithosphere emerges out of phase changes and does not necessitate partial melt as pointed out by Stixrude and Lithgow-Bertelloni [40]. Our results show the abrupt discontinuity around 410–420 km depth, with a better agreement with ak135 than PREM (best fit obtained with the "Stx" composition). It corresponds to the formation of wadsleyite ("Stx" and "Rng" compositions) or the disappearance of olivine ("Sax"

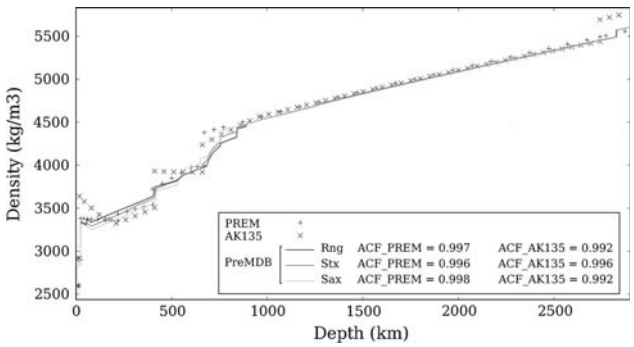

Fig. 2 Density-depth profile of PreMDB compared to the seismic models PREM and ak135

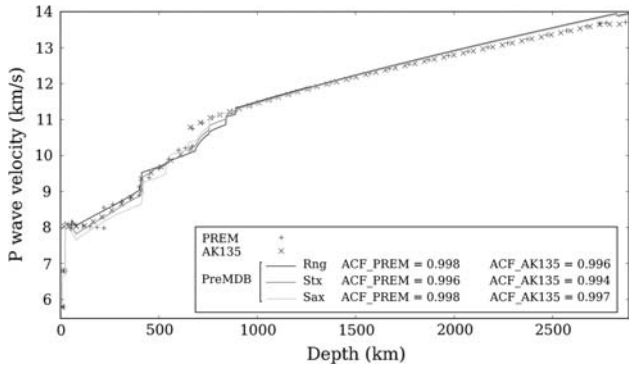

Fig. 3 V_P-depth profile of PreMDB compared to the seismic models PREM and ak135

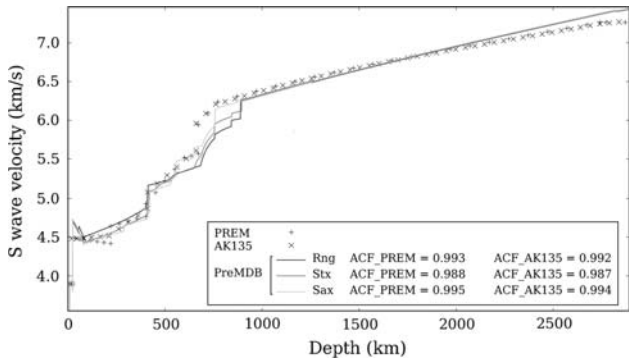

Fig. 4 V_S-depth profile of PreMDB compared to the seismic models PREM and ak135

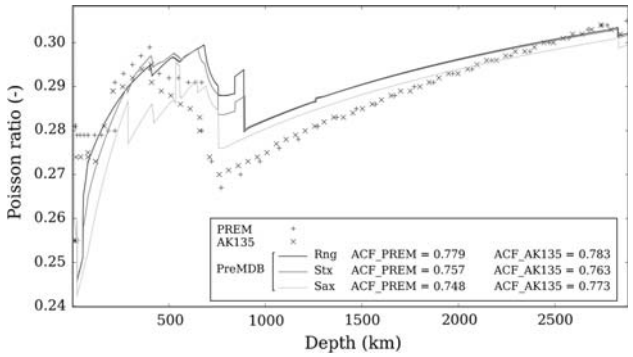

Fig. 5 Poisson's ratio profile of PreMDB compared to the seismic models PREM and ak135

composition). This result is in good agreement with seismological studies [3, 13, 22]. The calculation also predicts two other seismic discontinuities around 536 and 565 km depth only in the case of a composition depleted in Al_2O_3 and CaO but enriched in FeO ("Sax"). They correspond to the formation of majorite that then transforms in akimotoite. This result fits seismic observations [2, 13] and suggests that heterogeneities in the upper mantle composition lead to the presence or absence of this seismic discontinuity. Another significant result is that in none of the chemical models considered, the 660 km discontinuity comes out as a sharp jump in physical properties. There is rather a series of phase changes in the 650–890 km depth range depending on the composition considered. This result differs from PREM and ak135 seismological data and may result from an incomplete description of the solid solutions considered in the thermodynamic model. The chemical composition and temperature profile considered, in particular the underlying equilibrium assumption, may also be responsible for this discrepancy. However, compositions depleted in Al_2O_3 and CaO but enriched in FeO [38] fit the jump more closely than the other compositions considered. The calculations predict the formation of perovskite at the detriment of akimotoite at 649 km depth, followed by the appearance of periclase at 697 km depth and finally the transformation of ringwoodite in magnesiowustite at 758 km depth. This result supports the hypothesis that the 660 km discontinuity is a transition zone as inferred by receiver function analyses [13, 44] and is thus in agreement with more recent observations than ak135 and PREM.

A third deviation of the model is observed in the lower mantle increasing towards the core-mantle boundary and particularly around 2,830–2,840 km depth that corresponds to the transformation of perovskite into post-perovskite. The deviation to the seismic data suggests that the pyrolite composition model may not accurately reflect the chemistry of the lowermost mantle. This observation supports the hypothesis that the lowermost mantle has a different chemical composition resulting possibly from an accumulation of subducted slabs [17]. Other parameters such as sub-adiabatic conditions in the lower mantle, anisotropy or iron spin transition could also be responsible for the shift observed in the lower mantle results.

An interesting observation is the discrepancy between simulated and seismological Poisson's ratio (autocorrelation functions respectively of 0.748–0.779 and 0.763–0.783 for PREM and ak135, depending on the pyrolitic composition considered—Fig. 5), especially around the 660 km discontinuity. This result shows that this parameter is very sensitive to chemistry variation. Therefore it can be a useful marker of the variation of mantle composition with depth and could be used for future fine tuning of mantle chemistry.

4 Discussion

Recent studies [40, 41] have shown that physical properties of terrestrial rocks and minerals derived from thermodynamic potentials complement geophysical observations and experimental measurements. In our benchmark study, the model fits the PREM and ak135 seismic models and may even record more precise discontinuities due to thermodynamically predicted of phase transitions. Discrepancies in the thermodynamic simulations may result from an incomplete description of the solid solutions considered in the thermodynamic model, as well as from the chemical composition and temperature profile considered, in particular the underlying equilibrium assumption. Another component of the uncertainties is that the PREM and ak135 seismic reference data derive from experimental measurements.

The properties of terrestrial rocks and minerals previously determined from laboratory analyses can now be derived more accurately from thermodynamic modelling for the entire temperature and pressure range of the Earth's mantle. An advantage of this approach is that it permits self-consistent extrapolation beyond the range of the laboratory. The computational tool we use for this purpose is Perple_X, a Gibbs energy minimisation algorithm that computes phase equilibria, maps phase relations and extracts mineral physical properties of geodynamical interest. Perple_X is robust and computes stable mineral assemblages. It computes the thermochemical, thermal, seismic and other elastic properties from fundamental thermodynamic relations. In particular, Perple_X predicts phase transitions that are important for seismic tomography and geodynamic modelling. In addition to input from

Perple_X, complementary transport properties derived from laboratory experiments were added to enhance the information for the user. The resulting reference material database is a foundation for performing realistic simulations of rock behaviour during geological and geodynamic processes.

5 Future work

A particularly useful addition for the PreMDB database is the incorporation of other transport properties such as plasticity and creep, or fluid permeability of solid rocks. This addition builds on the capability of PreMDB to incorporate and visualize empirical data sets. This work is in progress. End-member flow laws such as olivine, quartz and feldspar dominated rocks are implemented as proxies for mantle, upper crust and lower crust, respectively. Quartz and olivine creep properties are implemented as a function of water fugacity.

We also intend to upgrade the PreMDB database in the future to implement more single mineral data and bulk composition models, with an effort to validate the individual solid solution models. Another focus will be the improved implementation of melts, melt solutions allowing the user to extract further melt properties. Other improvements consider the implementation of a new GUI for pseudosections to allow stacking of layers of individual phases. We will also apply PreMDB by coupling it with finite element models to run geological, geotechnical and geodynamical models driven by chemistry and heat.

Acknowledgments This work is a contribution to IGCP 557. The authors would like to acknowledge the support by the Western Australian Government, through the Premiers Fellowship Program and the Minerals Downunder Flagship CSIRO, The University of Western Australia as well as the *pmd* × *CRC*.

References

1. Behn MD, Kelemen PB (2003) Relationship between seismic P-wave velocity and the composition of anhydrous igneous and meta-igneous rocks. Geochem Geophys Geosyst 4(5):1–57
2. Bina CR (1991) Mantle discontinuities. Rev Geophys 29:783–793
3. Bina CR (1998) Mantle mineralogy—Olivine emerges from isolation. Nature. 392(6677):650–+
4. Bina CR (1998) A note on latent heat release from disequilibrium phase transformations and deep seismogenesis. Earth Planets Space 50(11–12):1029–1034
5. Bina CR, Wood BJ (1987) Olivine-spinel transitions—experimental and thermodynamic constraints and implications for the nature of the 400-Km seismic discontinuity. J Geophys Res-Solid 92(B6):4853–4866
6. Cammarano F, Goes S, Vacher P, Giardini D (2003) Inferring upper-mantle temperatures from seismic velocities. Phys Earth Planet Int 138(3–4):197–222
7. Clauser C, Huenges E (1995) Thermal conductivity of rocks and minerals in rock physics and phase relations—a handbook of physical constants, A.R.S. 3, Editor
8. Connolly JAD (1990) Multivariable phase-diagrams—an algorithm based on generalized thermodynamics. Am J Sci 290(6):666–718
9. Connolly JAD (2005) Computation of phase equilibria by linear programming: a tool for geodynamic modeling and its application to subduction zone decarbonation. Earth Planet Sci Lett 236(1–2):524–541
10. Connolly JAD, Kerrick DM (2002) Metamorphic controls on seismic velocity of subducted oceanic crust at 100–250 km depth. Earth Planet Sci Lett 204(1–2):61–74
11. Connolly JAD, Petrini K (2002) An automated strategy for calculation of phase diagram sections and retrieval of rock properties as a function of physical conditions. J Metamorph Geol 20(7):697–708
12. Deschamps F, Trampert J (2004) Towards a lower mantle reference temperature and composition. Earth Planet Sci Lett 222(1):161–175
13. Deuss A, Redfern SAT, Chambers K, Woodhouse JH (2006) The nature of the 660-kilometer discontinuity in Earth's mantle from global seismic observations of PP precursors. Science 311(5758):198–201
14. Duffy TS, Anderson DL (1989) Seismic velocities in mantle minerals and the mineralogy of the upper mantle. J Geophys Res-Solid 94(B2):1895–1912
15. Dziewonski AM, Anderson DL (1981) Preliminary reference earth model. Phys Earth Planet Int 25(4):297–356
16. Ghiorso MS, Sack RO (1995) Chemical mass-transfer in magmatic processes. 4. A revised and internally consistent thermodynamic model for the interpolation and extrapolation of liquid-solid equilibria in magmatic systems at elevated-temperatures and pressures. Contrib Mineral Petrol 119(2–3):197–212
17. Grand SP (2002) Mantle shear-wave tomography and the fate of subducted slabs. Philoso Trans Royal Soc Lond Ser Math Phys Eng Sci 360(1800):2475–2491
18. Hart SR, Zindler A (1986) In search of a bulk-earth composition. Chem Geol 57(3–4):247–267
19. Holland T, Powell R (1998) An internally consistent thermodynamic data set for phases of petrological interest. J Metamorph Geol. 16:309–343
20. Hoschek G (2004) Comparison of calculated P-T pseudosections for a kyanite eclogite from the Tauern Window, Eastern Alps, Austria. Eur J Miner 16(1):59–72
21. Hui H, Zhang Y (2007) Toward a general viscosity equation for natural anhydrous and hydrous silicate melts. Geochim Cosmochim Acta 71:403–416
22. Irifune T, Isshiki M (1998) Iron partitioning in a pyrolite mantle and the nature of the 410-km seismic discontinuity. Nature 392(6677):702–705
23. Irifune T, Ringwood AE (1987) Phase-transformations in a harzburgite composition to 26 Gpa—implications for dynamical behavior of the subducting slab. Earth Planet Sci Lett 86(2–4):365–376
24. Ita J, Stixrude L (1992) Petrology, elasticity, and composition of the mantle transition zone. J Geophys Res-Solid Earth 97(B5):6849–6866
25. Karki BB, Stixrude L, Wentzcovitch RM (2001) High-pressure elastic properties of major materials of Earth's mantle from first principles. Rev Geophys 39(4):507–534
26. Kennett BLN, Engdahl ER, Buland R (1995) Constraints on seismic velocities in the earth from travel-times. Geophys J Int 122(1):108–124
27. Khan A, Connolly JAD, Olsen N (2006) Constraining the composition and thermal state of the mantle beneath Europe from

inversion of long-period electromagnetic sounding data. J Geophys Res-Solid Earth 111:B10
28. Klein EM, Langmuir CH (1987) Global correlations of ocean ridge basalt chemistry with axial depth and crustal thickness. J Geophys Res 92:8089–8115
29. Matas J, Bass J, Ricard Y, Mattern E, Bukowinski MSI (2007) On the bulk composition of the lower mantle: predictions and limitations from generalized inversion of radial seismic profiles. Geophys J Int 170:764–780
30. Mattern E, Matas J, Ricard Y, Bass J (2005) Lower mantle composition and temperature from mineral physics and thermodynamic modelling. Geophys J Int 160(3):973–990
31. McKenzie D, Bickle MJ (1988) The volume and composition of melt generated by extension of the lithosphere. J Petrol 29:625–679
32. Montagner JP, Kennett BLN (1996) How to reconcile body-wave and normal-mode reference earth models. Geophys J Int 125(1):229–248
33. Ozkahraman HT, Selver R, Isik EC (2004) Determination of the thermal conductivity of rock from P-wave velocity. Int J Rock Mech Miner 41(4):703–708
34. Plank T, Langmuir CH (1998) The chemical composition of subducting sediment and its consequences for the crust and mantle. Chem Geol 145:325–394
35. Ringwood AE (1979) Origin of the Earth and Moon. Springer, New York
36. Ringwood AE (1991) Phase-transformations and their bearing on the constitution and dynamics of the mantle. Geochim Cosmochim Acta 55(8):2083–2110
37. Rudnick RL, Fountain DM (1995) Nature and composition of the continental crust: a lower crustal perspective. Rev Geophys 33(3):267–309
38. Saxena SK (1996) Earth mineralogical model: Gibbs free energy minimization computation in the system MgO-FeO-SiO2. Geochim Cosmochim Acta 60(13):2379–2395
39. Staudigel H, Plank T, White B, Schmincke H-U (1996) Geochemical fluxes during seafloor alteration of the basaltic upper ocean crust: DSDP 417 and 418. In: Bebout GE et al (eds) Subduction: top to bottom, American Geophysical Union Washington, pp 19–38
40. Stixrude L, Lithgow-Bertelloni C (2005) Mineralogy and elasticity of the oceanic upper mantle: origin of the low-velocity zone. J Geophys Res-Solid Earth 110:B03204
41. Stixrude L, Lithgow-Bertelloni C (2005) Thermodynamics of mantle minerals—I. Physical properties. Geophys J Int 162(2):610–632
42. Taylor SR, McLennan M (1985) The continental crust: its composition and evolution: an examination of the geochemical record preserved in sedimentary rocks. Blackwell, Oxford, p 312
43. Trampert J, Vacher P, Vlaar N (2001) Sensitivities of seismic velocities to temperature, pressure and composition in the lower mantle. Phys Earth Planet Int 124(3–4):255–267
44. Vacher P, Mocquet A, Sotin C (1998) Computation of seismic profiles from mineral physics: the importance of the non-olivine components for explaining the 660 km depth discontinuity. Phys Earth Planet In 106(3–4):275–298
45. Watt JP, Davies GF, Oconnell RJ (1976) Elastic properties of composite-materials. Rev Geophys 14(4):541–563
46. Weidner DJ (1985) A mineral physics test of a pyrolite mantle. Geophys Res Lett 12(7):417–420
47. Zoth G, Hanel R (1988) Appendix. In: Hanel R, Stegena L, Rybach L (eds) Handbook of terrestrial heat-flow density determination. Kluwer, Dordrecht, pp 449–466